Progress In Electromagnetics Research, Vol. 132, 25–48, 2012

A MATRIX SPLITTING DDM BASED ON SVE-BI FOR MULTIPLE CONDUCTING BODIES COATED BY THIN LAYER DIELECTRIC

L. Lei, J. Hu*, and H.-Q. Hu

School of Electronic Engineering, University of Electronic Science and Technology of China, Chengdu 611731, China

Abstract—A matrix splitting domain decomposition method based on hybrid shell vector element–boundary integral (MSDD-SVE-BI) for three dimensional electromagnetic scattering from multiple conducting bodies coated by thin layer dielectric is proposed. In the framework of domain decomposition, the whole computational domains are divided into a lot of sub-SVE-domains and boundary element domains. For conducting body coated with thin-layer dielectric, the shell vector element is used instead of traditional tetrahedral elements to reduce the number of unknowns. Further, a block Gauss-Seidel type preconditioner is applied to attain fast matrix splitting formulation for the matrix connecting surface electric field and surface magnetic field. By this method, only sub-matrix inversion is required in the SVE-BI method, the computational time for connecting matrix can be reduced greatly. Several numerical examples prove the accuracy and efficiency of the present method.

1. INTRODUCTION

Recently, electromagnetic scattering from single or multiple conducting bodies coated by thin-layer dielectric has attracted more and more interests. Typical applications can be found in microwave integrated circuits design, antenna array design, analysis of stealth objects and so on.

For conductor structures coated by thin-layer material, many numerical methods have been developed up to now. These numerical methods can be divided two categories. The first category is accurate boundary condition based method, including finite-difference

Received 30 June 2012, Accepted 30 August 2012, Scheduled 21 September 2012

* Corresponding author: Jun Hu (hujun@uestc.edu.cn).

time-domain, integral equation method, hybrid finite element with boundary integral method. The conformal finite-difference time-domain (CFDTD) approach is developed to compute scattering from anisotropically coated bodies in [1]. The CFDTD method based on effective constitutive parameters is presented to simulate the electromagnetic scattering of targets with thin-coating accurately [2]. The surface integral equation (SIE) method has been developed for scattering from arbitrary shaped conducting bodies coated with lossy materials of arbitrary thickness in [3]. But for thin coating problems, the SIE method is very difficult to converge into correct numerical solutions due to very ill-posed matrix. The finite element method (FEM) is widely used for modeling of composite conducting body and dielectric because of its powerful ability of modeling inhomogeneous materials [4]. In order to combine together the advantage of FEM and boundary integral method, the hybrid FEM with boundary integral method (FEM-BI) is proposed [5–7]. Though the FEM-BI has a good computational property for composite conducting body and dielectric, it is deficient for analysis of conductor structures coated by thin-layer material because a great deal of volume elements are required.

The second category for thin-coating problems is approximate boundary condition based method, it realizes efficient solution by simplifying electromagnetic analysis, including the impedance boundary condition (IBC) [8], thin dielectric sheet (TDS) approximation [9–12]. These methods avoid the volumetric discretization of material region, the computational region is only limited as the surface of conductor. A multilevel-TDS extension is also proposed for solution of conducting body coated by multi-thin-layer materials [13, 14].

Recently, shell vector element (SVE) has been paid much attention because of its good performance for modeling of thin materials [15, 16]. As a degenerated prism element, the SVE belongs to the second category mentioned above, a specific field distribution along normal direction in material region is assumed. Based on the SVE, the volume integration can be simplified into surface integration, and fewer elements are required compared with traditional tetrahedral elements. In [17], hybrid shell vector element–boundary integral method (SVE-BI) is developed by us to analyze the scattering of conducting body coated by single thin layer material and multiple thin layers materials.

To realize efficient analysis of the scattering from multiple objects, we resort to domain decomposition method (DDM). This is because the entire region related to the problem is huge especially when the separation distance between each object is electrically large, enormous number of unknowns is required. The DDM makes it possible by the strategy of "divide and conquer". A DDM based on the FEM-BI

framework is presented in [18] to analyze the scattering of multiple objects. A DDM based on an iterative sub-structuring method is used to solve the scattering by multiple objects [19]. A systematic research on domain decomposition method for solving electrically large electromagnetic problems is also done in [20].

In this paper, a hybrid matrix splitting DDM with SVE-BI (MSDDM-SVE-BI) is developed for multiple conducting bodies coated by thin layer dielectric. By use of a block Gauss-Seidel type pre-conditioner, no iterative or inverse operation for the original matrix of sub-SVE-domains is required for computation of connecting matrix, the computational time can be reduced greatly. The rest of paper is organized as follows: Firstly, the principle of a MSDDM-SVE-BI method for single conducting body coated by thin layer dielectric is introduced in Section 2. The extension of MSDDM-SVE-BI into multiple conducting bodies coated by thin layer dielectric is presented in Section 3. Finally, several examples are given to demonstrate the efficiency and accuracy of the present method. Finally the conclusions are also given.

2. THE MATRIX SPLITTING DDM FOR SINGLE CONDUCTING BODY COATED BY THIN LAYER DIELECTRIC

The scattering problem of single conducting body coated by thin layer dielectric is shown in Fig. 1. The object is illuminated by an incident wave $\mathbf{E}^{inc}$ or $\mathbf{H}^{inc}$, the $\hat{n}$ is the unit normal vector on surface of the object. $\mathbf{J}_u$ and $\mathbf{M}_u$ are the equivalent surface electric and magnetic currents on the coating dielectric surface.

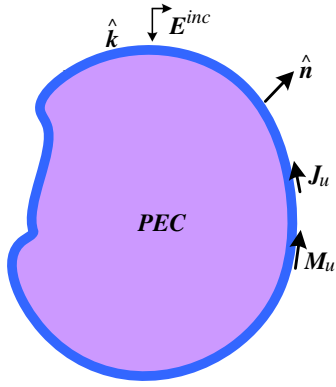

Figure 1. The scattering problem of single conducting body coated by thin layer dielectric.

The **E** field inside the coating dielectric satisfies the following equation:

$$\pounds \mathbf{E} = 0 \tag{1}$$

where $\pounds = \boldsymbol{\nabla} \times (\boldsymbol{\mu}_r^{-1} \boldsymbol{\nabla} \times) - k_0^2 \boldsymbol{\varepsilon}_r$, $\boldsymbol{\mu}_r$, $\boldsymbol{\varepsilon}_r$ denotes the relative permeability and permittivity of coating dielectric, respectively. k_0 is the wave number in free space.

Because the tangential electric field and tangential magnetic field is continuous on the boundary, the boundary conditions on the surface of coating dielectric **S** are written as:

$$\hat{n} \times \mathbf{E}\,|_{S^-} = \hat{n} \times \mathbf{E}\,|_{S^+} \tag{2}$$

$$\hat{n} \times \left(\frac{1}{\boldsymbol{\mu}_r} \nabla \times \mathbf{E} \right) |_{S^-} = -jk_0 \hat{n} \times \bar{\mathbf{H}}\,|_{S^+} \tag{3}$$

where $\bar{\mathbf{H}} = \eta_0 \mathbf{H}$, η_0 is the wave impedance in free space.

According to the general variational principle, the functional $F(\mathbf{E})$ can be written as [4]:

$$F(\mathbf{E}) = \frac{1}{2} \langle \pounds \mathbf{E}, \mathbf{E} \rangle - \frac{1}{2} \langle \pounds \mathbf{E}, \mathbf{u} \rangle + \frac{1}{2} \langle \mathbf{E}, \pounds \mathbf{u} \rangle \tag{4}$$

where **u** is an arbitrary vector which satisfies the boundary condition (2) and (3).

The arbitrary vector **u** is eliminated when we construct the functional $F(\mathbf{E})$ based on Equation (4), and the boundary conditions on the surface of coating dielectric **S** Equation (2) and Equation (3), the functional $F(\mathbf{E})$ is expressed as follows [4]:

$$\begin{aligned} F(\mathbf{E}) = {} & \frac{1}{2} \iiint_V \left[\frac{1}{\boldsymbol{\mu}_r} (\nabla \times \mathbf{E}) \cdot (\nabla \times \mathbf{E}) - k_0^2 \boldsymbol{\varepsilon}_r \mathbf{E} \cdot \mathbf{E} \right] \mathbf{dV} \\ & + \mathbf{j} k_0 \boldsymbol{\eta}_0 \iint_S \hat{\mathbf{n}} \cdot (\mathbf{E} \times \mathbf{H}_s) \mathbf{dS} \end{aligned} \tag{5}$$

For dielectric region, the vector tetrahedral element is usually used as a volume basis function to expand the electric field as:

$$\mathbf{E} = \sum_{j=1}^{6} E_j^e \mathbf{N}_\mathbf{j}^e \tag{6}$$

where the basis function of the jth edge $\mathbf{N}_\mathbf{j}^e = (L_{j1}^e \nabla L_{j2}^e - L_{j2}^e \nabla L_{j1}^e) \mathbf{l}_j^e$, $j1$ and $j2$ are the node of the jth edge of the tetrahedral element respectively; L_{j1}^e and L_{j2}^e are the normalized volume of the tetrahedral element; $\mathbf{l}_j^e$ is the length of the jth edge of the tetrahedral element; E_j^e is the unknown coefficient.

For the surface integral term in Equation (5), the magnetic field on the surface of coating dielectric can be expanded by three edges of planar triangle on surface **S** as:

$$\mathbf{H}_s = \sum_{j=1}^{3} H_j^s \mathbf{N}_\mathbf{j}^s \tag{7}$$

where the basis function of the jth edge $\mathbf{N}_\mathbf{j}^s = (L_{j1}^s \nabla L_{j2}^s - L_{j2}^s \nabla L_{j1}^s)\mathbf{l}_j^s$, $j1$ and $j2$ are the node of the jth edge of triangle element respectively; L_{j1}^s and L_{j2}^s are the normalized area of triangle element; $\mathbf{l}_j^s$ is the length of the jth edge; H_j^s is the unknown coefficient.

The FEM matrix can be written as:

$$[\mathbf{K}]\{E\} - [\mathbf{B}]\{H\} = \{0\} \tag{8}$$

The representation of matrix **K**, **B** can be easily derived as follows:

$$K_{ij} = \frac{1}{2}\iiint_V \left[\frac{1}{\boldsymbol{\mu}_r}(\nabla \times \mathbf{N}_i)\cdot(\nabla \times \mathbf{N}_j) - k_0^2 \boldsymbol{\varepsilon}_r \mathbf{N}_i \cdot \mathbf{N}_j\right]\mathbf{dV} \tag{9}$$

$$B_{ij} = \mathbf{j}k_0\boldsymbol{\eta}_0 \iint_S \hat{\mathbf{n}}\cdot(\mathbf{N}_i \times \mathbf{N}_j)\mathbf{dS} \tag{10}$$

For thin layer material, a great deal of elements are required in traditional discretization. To realize efficient solution of thin layer material, the shell vector element can be used.

As shown in Fig. 2, there are six edge vectors along the corresponding edges in the upper triangle and bottom triangle, and three normal vectors. A linear function $\beta(\boldsymbol{\varsigma})$ was used to describe the variation of the field along the normal direction, and $\nabla\beta = -\frac{\hat{\mathbf{n}}}{d}$.

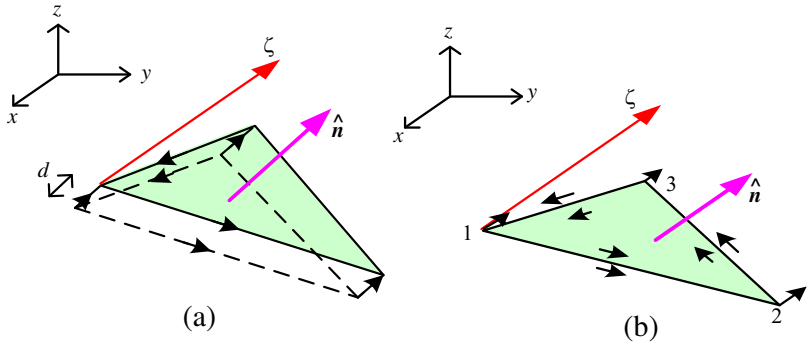

Figure 2. The structure of the prism element and the shell element. (a) The prism element. (b) The shell element.

The $\beta\mathbf{N}_j (j = 1, 2, 3)$, $\beta'\mathbf{N}'_j (j = 1, 2, 3)$ are the edge basis functions in the upper and bottom triangle respectively. The $L_j, j = 1, 2, 3$ is the normal basis function at the node-j.

By the SVE, the electric field is expanded as follows [16, 17]:

$$\mathbf{E}^e = \sum_{j=1}^{3} \left(E^e_{u_j} \boldsymbol{\beta} \mathbf{N}_j + E^e_{bj} \boldsymbol{\beta}' \mathbf{N}'_j \right) + \sum_{j=1}^{3} E^e_{nj} L^e_j \hat{\mathbf{n}} \tag{11}$$

where

$$\begin{aligned} \beta' &= 1 - \beta, \\ \mathbf{N}_j &= \left(L^e_{j1} \nabla L^e_{j2} - L^e_{j2} \nabla L^e_{j1} \right) \mathbf{l}^e_j, \\ \mathbf{N}'_j &= \left(L^e_{j1} \nabla L^e_{j2} - L^e_{j2} \nabla L^e_{j1} \right) \mathbf{l}^e_j \end{aligned}$$

$\mathbf{E}^e_{u_j}$: the expansion coefficient of the jth edge vector in upper triangle

$\mathbf{E}^e_{b_j}$: the expansion coefficient of the jth edge vector in bottom triangle

$\mathbf{E}^e_{nj}$: the expansion coefficient of normal vector at the node-j

$\mathbf{l}^e_j$: the length of the jth edge

With the shell vector element, Equation (8) can be written as:

$$\begin{aligned} &\iiint_V \left\{ \nabla \times \left[\beta \mathbf{N}^e_i + \beta' \mathbf{N}^e_i + L^e_i \hat{n} \right] \cdot \nabla \right. \\ &\times \boldsymbol{\mu}_r^{-1} \left[\sum_{j=1}^{3} \left(\mathbf{E}^e_{uj} \beta \mathbf{N}^e_j + \mathbf{E}'^e_{uj} \beta' \mathbf{N}^e_j \right) + \sum_{j=1}^{3} \mathbf{E}^e_{dj} L^e_j \hat{n} \right] - k_0^2 \boldsymbol{\varepsilon}_r \\ &\left. \left[\beta \mathbf{N}^e_i + \beta' \mathbf{N}^e_i + L^e_i \hat{n} \right] \cdot \left[\sum_{j=1}^{3} \left(\mathbf{E}^e_{uj} \beta \mathbf{N}^e_j + \mathbf{E}'^e_{uj} \beta' \mathbf{N}^e_j \right) + \sum_{j=1}^{3} \mathbf{E}^e_{dj} L^e_j \hat{n} \right] \right\} dV \\ = \; & j k_0 \eta_0 \sum_{j=1}^{3} \mathbf{H}^s_{uj} \iint_s \mathbf{N}^s_i \cdot \left(\hat{n} \times \mathbf{N}^s_j \right) ds \end{aligned} \tag{12}$$

For the shell element model, by using $\nabla \beta = -\frac{\hat{\mathbf{n}}}{d}$ and $dV = d\varsigma dS$,

the volume integral can be simplified as surface integral, for example,

$$\iiint_V (\nabla\times\beta\mathbf{N}_i^e)\cdot\boldsymbol{\mu}_r^{-1}\left(\nabla\times\beta'\mathbf{N}_j^e\right)dV = \int_{-\frac{1}{2}}^{\frac{1}{2}}\beta\beta' d\varsigma\iint_s(\nabla\times\mathbf{N}_i^e)\cdot\boldsymbol{\mu}_r^{-1}\left(\nabla\times\mathbf{N}_j^e\right)$$
$$dS+\int_{-\frac{1}{2}}^{\frac{1}{2}}\frac{\beta}{d}d\varsigma\iint_s(\nabla\times N_i^e)\cdot\boldsymbol{\mu}_r^{-1}\mathbf{S}_j^e dS-\int_{-\frac{1}{2}}^{\frac{1}{2}}\frac{\beta'}{d}d\varsigma\iint_s\mathbf{S}_i^e\boldsymbol{\mu}_r^{-1}\left(\nabla\times N_j^e\right)dS$$
$$-\int_{-\frac{1}{2}}^{\frac{1}{2}}\frac{1}{d^2}d\varsigma\iint_s\mathbf{S}_i^e\cdot\boldsymbol{\mu}_r^{-1}S_j^e dS=\frac{d}{6}\iint_s(\nabla\times\mathbf{N}_i^e)\cdot\boldsymbol{\mu}_r^{-1}\left(\nabla\times\mathbf{N}_j^e\right)dS$$
$$+\frac{1}{2}\iint_s(\nabla\times\mathbf{N}_i^e)\cdot\boldsymbol{\mu}_r^{-1}\mathbf{S}_j^e dS-\frac{1}{2}\iint_s S_i^e\boldsymbol{\mu}_r^{-1}(\nabla\times\mathbf{N}_j^e)dS$$
$$-\frac{1}{d}\iint_s\mathbf{S}_i^e\cdot\boldsymbol{\mu}_r^{-1}\mathbf{S}_j^e dS \tag{13}$$

$$\begin{aligned}\iiint_V k_0^2\beta\beta'\mathbf{N}_i^e\cdot\boldsymbol{\varepsilon}_r\mathbf{N}_j^e dV &= k_0^2\int_{-\frac{1}{2}}^{\frac{1}{2}}\beta\beta' d\varsigma\iint_s\mathbf{N}_i^e\cdot\boldsymbol{\varepsilon}_r\mathbf{N}_j^e dS\\ &= k_0^2\frac{d}{6}\iint_s\mathbf{N}_i^e\cdot\boldsymbol{\varepsilon}_r\mathbf{N}_j^e dS\end{aligned} \tag{14}$$

$$\iiint_V(\nabla\times L_i^e\hat{n})\cdot\boldsymbol{\mu}_r^{-1}\left(\nabla\times\beta'\mathbf{N}_j^e\right)dV=\int_{-\frac{1}{2}}^{\frac{1}{2}}\beta' d\varsigma\iint_s(\nabla L_i^e\times\hat{n})\cdot\boldsymbol{\mu}_r^{-1}$$
$$\left(\nabla\times\mathbf{N}_j^e\right)dS+\int_{-\frac{1}{2}}^{\frac{1}{2}}\frac{1}{d}d\varsigma\iint_s(\nabla L_i^e\times\hat{n})\cdot\boldsymbol{\mu}_r^{-1}\mathbf{S}_j^e dS$$
$$=\frac{d}{2}\iint_s(\nabla L_i^e\times\hat{n})\cdot\boldsymbol{\mu}_r^{-1}\left(\nabla\times\mathbf{N}_j^e\right)dS+\iint_s(\nabla L_i^e\times\hat{n})\cdot\boldsymbol{\mu}_r^{-1}\mathbf{S}_j^e dS \tag{15}$$

where $\mathbf{S}_i^e=\hat{\mathbf{n}}\times\mathbf{N}_i^e$, $\mathbf{S}_j^e=\hat{\mathbf{n}}\times\mathbf{N}_j^e$, d is the thickness of the thin-layer dielectric.

In the FEM-BI method, the SIE is applied on the surface $\mathbf{S}$. The electric field integral equation (EFIE) and the magnetic field integral equation (MFIE) are used as follows,

$$\mathbf{E}^{inc} = L(\bar{\mathbf{J}})-K(\mathbf{M}) \tag{16}$$
$$\bar{\mathbf{H}}^{inc} = K(\bar{\mathbf{J}})+L(\mathbf{M}) \tag{17}$$

The equivalent surface electric and magnetic currents are defined as:

$$\mathbf{J} = \hat{\mathbf{n}}\times\mathbf{H} \tag{18}$$
$$\mathbf{M} = \mathbf{E}\times\hat{\mathbf{n}} \tag{19}$$
$$\bar{\mathbf{J}} = \hat{\mathbf{n}}\times\bar{\mathbf{H}} \tag{20}$$

here $\bar{\mathbf{H}}^{inc} = \boldsymbol{\eta}_0 \mathbf{H}^{inc}$. The integral operator L, K are expressed as, respectively,

$$L(\mathbf{X}) = \mathbf{j}\mathbf{k}_0 \int_{s'} \left[\mathbf{X}\left(\mathbf{r}'\right) + \frac{1}{k_0^2} \nabla\nabla' \cdot \mathbf{X}\left(\mathbf{r}'\right) \right] \mathbf{G}\left(\mathbf{r}, \mathbf{r}'\right) \mathbf{ds}' \tag{21}$$

$$K(\mathbf{X}) = T\mathbf{Y}(\mathbf{r}) + \int_{s'} \mathbf{X}(\mathbf{r}') \times \nabla \mathbf{G}(\mathbf{r}, \mathbf{r}') \mathbf{ds}' \tag{22}$$

In Equation (22), $\mathbf{Y}(\mathbf{r}) = \mathbf{X}(\mathbf{r}) \times \hat{\mathbf{n}}$, $T = 1 - \frac{\Omega}{4\pi}$. For the smooth surface, $\Omega = 2\pi$. $\mathbf{G} = \frac{e^{-jk_0|r-r'|}}{4\pi|\mathbf{r}-\mathbf{r}'|}$ is the Green's function in free space. The integral terms with bars in Equation (22) denote principal value integrals.

For the SIE on the surface $\mathbf{S}$, there are different formulations based on the EFIE (16) and the MFIE (17). For different combination of EFIE and MFIE, the condition number of final SIE matrix is also different. Here, the TENENH type SIE [7] is used to attain accurate numerical results due to its well-posed property. And, it can avoid the interior resonance occurred in some cases.

By choosing $\mathbf{S}_i^s = \hat{\mathbf{n}} \times \mathbf{N}_i$ as the weighting function of the EFIE, the tangential electric-field integral equation (TE: $\hat{\mathbf{t}} \cdot \mathbf{E}$) can be derived as

$$\left[\mathbf{P}^{TE}\right] \{E_u\} + \left[\mathbf{Q}^{TE}\right] \{H_u\} = \left\{\mathbf{b}^{TE}\right\} \tag{23}$$

where,

$$\begin{aligned} P_{ij}^{TE} &= -\int_S \mathbf{S}_i^s \cdot K(\mathbf{N}_j \times \hat{\mathbf{n}}) ds, \\ Q_{ij}^{TE} &= \int_S \mathbf{S}_i^s \cdot L(\boldsymbol{\eta}_0 \hat{\mathbf{n}} \times \mathbf{N}_j) ds, \\ b_i^{TE} &= \int_S \mathbf{S}_i^s \cdot \mathbf{E}^i ds \end{aligned}$$

Similarly, the $\hat{\mathbf{n}}$ crossed electric field integral equation (NE: $\hat{\mathbf{n}} \times \mathbf{E}$) can be derived by choosing $\hat{\mathbf{n}} \times \mathbf{S}_i^s$ as the weighting function of the EFIE,

$$\left[\mathbf{P}^{NE}\right] \{E_u\} + \left[\mathbf{Q}^{NE}\right] \{H_u\} = \left\{\mathbf{b}^{NE}\right\} \tag{24}$$

The tangential magnetic field integral equation (TH: $\hat{\mathbf{t}} \cdot \mathbf{H}$) can be derived by choosing $\mathbf{S}_i^s$ as the weighting function of the MFIE

$$\left[\mathbf{P}^{TH}\right] \{E_u\} + \left[\mathbf{Q}^{TH}\right] \{H_u\} = \left\{\mathbf{b}^{TH}\right\} \tag{25}$$

The $\hat{\mathbf{n}}$ crossed magnetic field integral equation (NH: $\hat{\mathbf{n}} \times \mathbf{H}$) can be derived by choosing $\hat{\mathbf{n}} \times \mathbf{S}_i^s$ as the weighting function of the MFIE:

$$\left[\mathbf{P}^{NH}\right] \{E_u\} + \left[\mathbf{Q}^{NH}\right] \{H_u\} = \left\{\mathbf{b}^{NH}\right\} \tag{26}$$

Based on the above equations, the TENENH type SIE is constructed as follows,

$$[\mathbf{P}]\{E_u\} + [\mathbf{Q}]\{H_u\} = \{\mathbf{b}\} \tag{27}$$

where,

$$\begin{aligned} [\mathbf{P}] &= \alpha\left[\mathbf{P}^{TE}\right] + \beta\left[\mathbf{P}^{NE}\right] + \gamma\left[\mathbf{P}^{NH}\right] \\ [\mathbf{Q}] &= \alpha\left[\mathbf{Q}^{TE}\right] + \beta\left[\mathbf{Q}^{NE}\right] + \gamma\left[\mathbf{Q}^{NH}\right] \\ \{\mathbf{b}\} &= \alpha\left\{\mathbf{b}^{TE}\right\} + \beta\left\{\mathbf{b}^{NE}\right\} + \gamma\left\{\mathbf{b}^{NH}\right\} \end{aligned} \tag{28}$$

The parameter α, β, γ satisfies: $\alpha+\beta+\gamma = 1$. More details about the TENENH type SIE can be found in [7].

Combining Equations (8) and (27), the matrix equation of SVE-BI is obtained:

$$\begin{bmatrix} \mathbf{K}_{dd} & -\mathbf{K}_{du} & 0 \\ -\mathbf{K}_{ud} & \mathbf{K}_{uu} & -\mathbf{B} \\ 0 & \mathbf{P} & \mathbf{Q} \end{bmatrix} \begin{Bmatrix} E_d \\ E_u \\ H_u \end{Bmatrix} = \begin{bmatrix} 0 \\ 0 \\ \mathbf{b} \end{bmatrix} \tag{29}$$

where E_d is the expansion coefficient of normal electric field at the mesh node, and the matrix dimension is $\mathbf{N}_d \times 1$. E_u is the expansion coefficient of electric field along the edge of upper triangle, and the matrix dimension is $\mathbf{N}_u \times 1$, because the bottom triangles locate on the surface of conducting body, so the value of E_u on the bottom triangles is zero. H_u is the expansion coefficient of magnetic field on the surface $\mathbf{S}$, and the matrix dimension is $\mathbf{N}_u \times 1$. $\mathbf{N}_d$ is the total number of normal vector unknowns at the mesh nodes. $\mathbf{N}_u$ is the total number of edge unknowns on the surface $\mathbf{S}$.

The Equation (8) can be written as:

$$\begin{bmatrix} \mathbf{K}_{dd} & -\mathbf{K}_{du} \\ -\mathbf{K}_{ud} & \mathbf{K}_{uu} \end{bmatrix} \begin{Bmatrix} \mathbf{E}_d \\ \mathbf{E}_u \end{Bmatrix} = \begin{bmatrix} 0 \\ \mathbf{B} \end{bmatrix} \{\mathbf{H}_u\} \tag{30}$$

where $\mathbf{K}_{dd}$ is a square matrix of $\mathbf{N}_d \times \mathbf{N}_d$. $\mathbf{K}_{du}$ is a matrix of $\mathbf{N}_d \times \mathbf{N}_u$. $\mathbf{K}_{ud}$ is a matrix of $\mathbf{N}_u \times \mathbf{N}_d$, $\mathbf{K}_{uu}$ is a square matrix of $\mathbf{N}_u \times \mathbf{N}_u$. $\mathbf{B}$ is a square matrix of $\mathbf{N}_u \times \mathbf{N}_u$.

Different from the DDM-FE-BI, no iterative or inverse operation for matrix $\mathbf{K}$ will be required here. With the aid of a block Gauss-Seidel type pre-conditioner [20], Equation (30) can be written as:

$$\begin{aligned} &\begin{bmatrix} \mathbf{K}_{dd} & 0 \\ -\mathbf{K}_{ud} & \mathbf{K}_{uu} \end{bmatrix}^{-1} \begin{bmatrix} \mathbf{K}_{dd} & -\mathbf{K}_{du} \\ -\mathbf{K}_{ud} & \mathbf{K}_{uu} \end{bmatrix} \begin{Bmatrix} \mathbf{E}_d \\ \mathbf{E}_u \end{Bmatrix} \\ = &\begin{bmatrix} \mathbf{K}_{dd} & 0 \\ -\mathbf{K}_{ud} & \mathbf{K}_{uu} \end{bmatrix}^{-1} \begin{bmatrix} 0 \\ \mathbf{B} \end{bmatrix} \{\mathbf{H}_u\} \end{aligned} \tag{31}$$

Because:

$$\begin{bmatrix} \mathbf{K}_{dd} & 0 \\ -\mathbf{K}_{ud} & \mathbf{K}_{uu} \end{bmatrix}^{-1} = \begin{bmatrix} \mathbf{K}_{dd}^{-1} & 0 \\ \mathbf{K}_{uu}^{-1}\mathbf{K}_{ud}\mathbf{K}_{dd}^{-1} & \mathbf{K}_{uu}^{-1} \end{bmatrix} \tag{32}$$

Equation (31) can be written as:

$$\begin{bmatrix} \mathbf{I} & -\mathbf{K}_{dd}^{-1}\mathbf{K}_{du} \\ 0 & \mathbf{I} - \mathbf{K}_{uu}^{-1}\mathbf{K}_{ud}\mathbf{K}_{dd}^{-1}\mathbf{K}_{du} \end{bmatrix} \begin{Bmatrix} \mathbf{E}_d \\ \mathbf{E}_u \end{Bmatrix} = \begin{bmatrix} 0 \\ \mathbf{K}_{uu}^{-1}\mathbf{B} \end{bmatrix} \{\mathbf{H}_u\} \tag{33}$$

$\mathbf{E}_u$ can be expressed as:

$$\{\mathbf{E}_u\} = \left\{\mathbf{I} - \mathbf{K}_{uu}^{-1}\mathbf{K}_{ud}\mathbf{K}_{dd}^{-1}\mathbf{K}_{du}\right\}^{-1} \mathbf{K}_{uu}^{-1}\mathbf{B}\,\{\mathbf{H}_u\} \tag{34}$$

Let $\{\mathbf{E}_u\} = \mathbf{X}_C \cdot \{\mathbf{H}_u\}$, so

$$\mathbf{X}_C = \left\{\mathbf{I} - \mathbf{K}_{uu}^{-1}\mathbf{K}_{ud}\mathbf{K}_{dd}^{-1}\mathbf{K}_{du}\right\}^{-1} \mathbf{K}_{uu}^{-1}\mathbf{B} \tag{35}$$

where $\mathbf{X}_C$ is a square matrix of $\mathbf{N}_u \times \mathbf{N}_u$, it connects the surface electric field $\mathbf{E}_u$ and surface magnetic field $\mathbf{H}_u$. From Equation (35), only sub-matrix inversion is required for $\mathbf{X}_C$.

Substituting Equation (35) into Equation (27), we have:

$$([\mathbf{P}]\,[\mathbf{X}_C] + [\mathbf{Q}\ ])\,[\mathbf{H}_u] = [\mathbf{b}] \tag{36}$$

In Equation (8), $\mathbf{K}$ is a square matrix of $(\mathbf{N}_d+\mathbf{N}_u)\times(\mathbf{N}_d+\mathbf{N}_u)$. By the matrix splitting domain decomposition based on hybrid shell vector element method–boundary integral (MSDD-SVE-BI), no iterative or inverse operation for matrix $\mathbf{K}$ is required. The dimension of the largest sub-matrix is only $\mathbf{N}_u \times \mathbf{N}_u$. The cost for sub-matrix $\mathbf{K}_{dd}$ and $\mathbf{K}_{uu}$ is far less than the one for whole matrix $\mathbf{K}$. Because total number of unknowns for thin layer dielectric is reduced greatly by the SVE, the MSDDM-SVE-BI is very suitable for analysis of multiple conducting bodies coated by thin layer dielectric.

3. MSDDM-SVE-BI FOR MULTIPLE CONDUCTING BODIES COATED BY THIN LAYER DIELECTRIC

The 3D electromagnetic scattering from multiple conducting bodies coated by thin layer dielectric is shown in Fig. 3. $\mathbf{J}_{u_m}$, $\mathbf{M}_{u_m}$ are the equivalent surface electric and magnetic currents on the mth surface. With DDM-SVE-BI, the concerning regions are the shell vector element regions of each object and the boundary element regions.

Because the sub-SVE matrix is independent for each object, the sub-SVE equation can be expressed independently. For the **m**th object, Equation (30) can be written as:

$$\begin{bmatrix} \mathbf{K}_{dd} & -\mathbf{K}_{du} \\ -\mathbf{K}_{ud} & \mathbf{K}_{uu} \end{bmatrix}_m \begin{Bmatrix} \mathbf{E}_{d_m} \\ \mathbf{E}_{u_m} \end{Bmatrix} = \begin{bmatrix} 0 \\ \mathbf{B} \end{bmatrix}_m \{\mathbf{H}_{u_m}\} \tag{37}$$

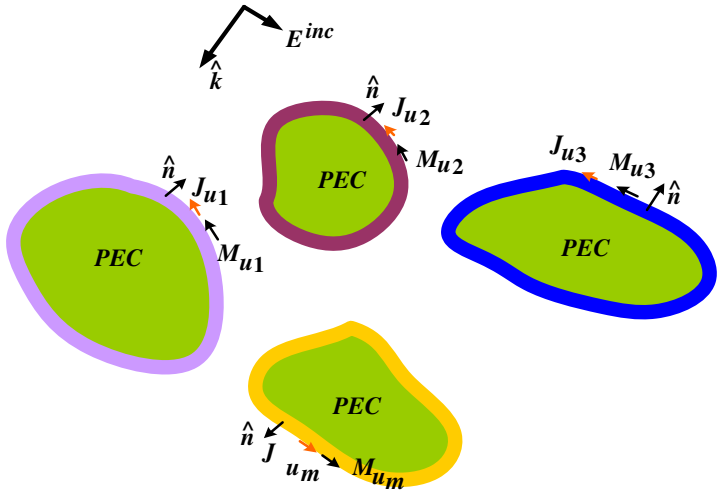

Figure 3. The scattering problem of multiple conducting bodies coated by thin layer dielectric materials.

where $\mathbf{E}_{d_m}$ is the expansion coefficient of normal electric field at the mesh node of the **m**th object, and the matrix dimension is $\mathbf{N}_{d_m} \times 1$. $\mathbf{E}_{u_m}$ is the expansion coefficient of tangential electric field along the upper triangle edge of the **m**th object, and the matrix dimension is $\mathbf{N}_{u_m} \times 1$. $\mathbf{H}_{u_m}$ is the expansion coefficient of tangential magnetic field on the **m**th object surface, and the matrix dimension is $\mathbf{N}_{u_m} \times 1$. $\mathbf{K}_{dd}$ is a square matrix of $\mathbf{N}_{d_m} \times \mathbf{N}_{d_m}$, $\mathbf{K}_{du}$ a matrix of $\mathbf{N}_{d_m} \times \mathbf{N}_{u_m}$, $\mathbf{K}_{ud}$ a matrix of $\mathbf{N}_{u_m} \times \mathbf{N}_{d_m}$, $\mathbf{K}_{uu}$ a square matrix of $\mathbf{N}_{u_m} \times \mathbf{N}_{u_m}$, $\mathbf{B}$ a square matrix of $\mathbf{N}_{u_m} \times \mathbf{N}_{u_m}$, $\mathbf{N}_{d_m}$ the number of normal unknowns at the mesh nodes of the **m**th object, and $\mathbf{N}_{u_m}$ the number of tangential edge unknowns of the **m**th object.

Similar to Equation (35), with a block Gauss-Seidel type preconditioner, after trivial derivation, we attain

$$\mathbf{X}_{C_m} = \left\{\mathbf{I} - \mathbf{K}_{uu}^{-1}\mathbf{K}_{ud}\mathbf{K}_{dd}^{-1}\mathbf{K}_{du}\right\}_m^{-1} \mathbf{K}_{uu_m}^{-1}\mathbf{B}_m \tag{38}$$

where $\mathbf{X}_{C_m}$ is a square matrix of $\mathbf{N}_{u_m} \times \mathbf{N}_{u_m}$.

Finally, the boundary integral equation for multiple objects is obtained:

$$([\mathbf{P}][\mathbf{X}_C] + [\mathbf{Q}])[\mathbf{H}_u] = [\mathbf{b}] \tag{39}$$

Where $[\mathbf{X}_C] = \begin{bmatrix} \mathbf{X}_{C_1} & 0 & \dots & 0 \\ 0 & \mathbf{X}_{C_2} & \dots & 0 \\ \dots & & & \\ 0 & 0 & \dots & \mathbf{X}_{C_m} \end{bmatrix}$, $[\mathbf{P}]$ and $[\mathbf{Q}]$ are square matrices of $\mathbf{N}_u \times \mathbf{N}_u$ and $\mathbf{H}_u$ a column matrix of $\mathbf{N}_u \times 1$. $\mathbf{N}_u =$

$\mathbf{N}_{u_1} + \mathbf{N}_{u_2} + \ldots \mathbf{N}_{u_m}$ denotes the summation of number of tangential edge unknowns of all objects.

As we know, the solution for $\mathbf{X}_{C_1}, \mathbf{X}_{C_2} \ldots, \mathbf{X}_{C_m}$ only relies on each SVE matrix. So the computation for $\mathbf{X}_{C_1}, \mathbf{X}_{C_2} \ldots, \mathbf{X}_{C_m}$ can be implemented in parallel. After attaining matrix $\mathbf{X}_C$, direct solver or iterative methods can be used to solve Equation (39).

4. NUMERICAL RESULTS

Several examples are given to prove the accuracy and efficiency of the matrix splitting domain decomposition method (MSDDM) based on the SVE-BI. The results by the analytical method, the DDM-FE-BI and the MSDDM-FE-BI method are used as comparisons, tetrahedral elements are used as volume elements in the DDM-FE-BI and MSDDM-FE-BI method.

4.1. Coating PEC Sphere

The first example is a coating PEC sphere, shown in Fig. 4. The frequency is 300 MHz. $k_0 a = 1$, the thickness of the coating layer $\boldsymbol{d}$ is $\frac{a}{30}$. The relative permittivity of coating dielectric is $\varepsilon_r = 4$. As shown in Fig. 5, the result of the MSDDM-SVE-BI coincides with the result of MIE method.

The comparison between MSDDM-FE-BI and MSDDM-SVE-BI for this problem is shown in Table 1, here mesh density is $\frac{\lambda_0}{15}$ for two methods. The number of unknowns is 290 in MSDDM-SVE-BI, but the one is 578 in MSDDM-FE-BI. This is because only normal unknown vectors are considered in dielectric region for MSDDM-SVE-BI. Obviously, the MSDDM-SVE-BI has less memory and time requirement than the MSDDM-FE-BI.

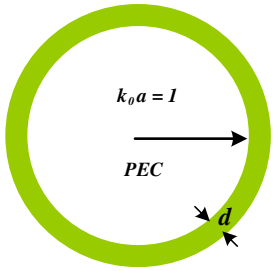

Figure 4. Coating PEC sphere.

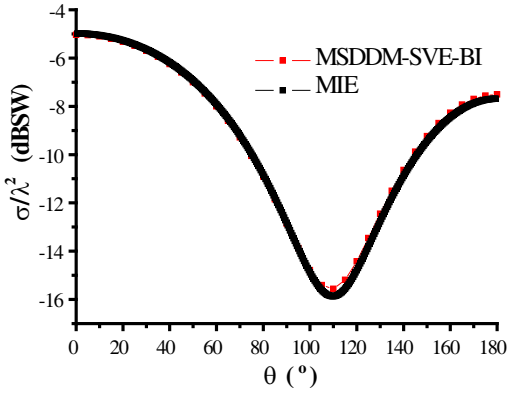

Figure 5. The bistatic RCS of coating PEC sphere.

Table 1. The comparison of MSDDM-SVE-BI and MSDDM-FE-BI. Bistatic RCS of a coating PEC sphere. (mesh density with $\frac{\lambda_0}{15}$). The sub-matrix $\mathbf{K}_{II}$, $\mathbf{K}_{bb}$ in FE-BI denotes the self-interaction matrix in coating dielectric region, on the surface of coating dielectric respectively.

Method	MSDDM-FE-BI
Unknowns	578
Memory of matrix K	1.05 Mb($\mathbf{K}_{II}$) /0.37 Mb($\mathbf{K}_{bb}$)

Method	MSDDM-SVE-BI
Unknowns	290
Memory of matrix K	0.044 Mb($\mathbf{K}_{dd}$)/0.37 Mb($\mathbf{K}_{uu}$)

4.2. Coating PEC Cube

The second example is a coating PEC cube. The geometry is shown in Fig. 6. The length of the cube is 0.1 m, the thickness of the coated layer is 0.001 m. The wavelength is 0.1 m. The incident angle of plane wave is $\theta^{inc} = 45°$, $\varphi^{inc} = 0°$. The bistatic RCS of the coating PEC cube is shown in Fig. 7. The results with MSDDM-SVE-BI agree well with the one by the commercial software FEKO.

The comparisons between MSDDM-SVE-BI and MSDDM-FE-BI for this problem are shown in Table 2, here mesh density is $\frac{\lambda_0}{10}$ for

two methods. The memory for two main sub-matrices $\mathbf{K}_{dd}$, $\mathbf{K}_{uu}$ are 5.2 Mb and 46.5 Mb respectively in MSDDM-SVE-BI, but the memory requirement of $\mathbf{K}_{II}$, $\mathbf{K}_{bb}$ in MSDDM-FE-BI is 68.96 Mb, 46.5 Mb respectively. Obviously, the computational time and memory requirement in MSDDM-SVE-BI is much less than the one in MSDDM-FE-BI.

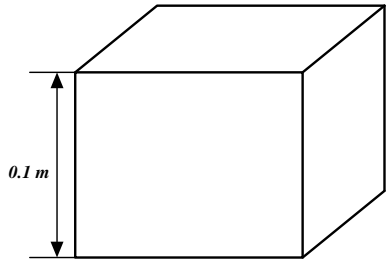

Figure 6. Coating PEC cube.

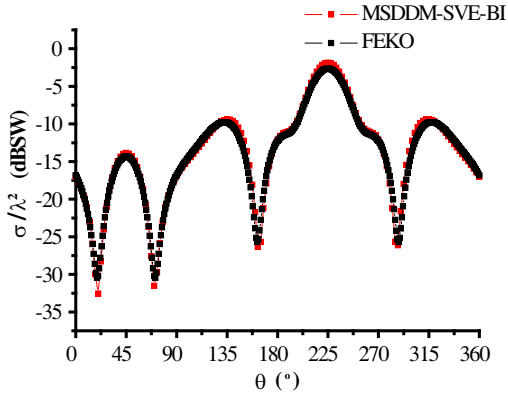

Figure 7. The bistatic RCS of coating PEC cube.

Table 2. The comparison of MSDDM-SVE-BI and MSDDM-FE-BI. Bistatic RCS of coating PEC cube. (mesh density with $\frac{\lambda_0}{10}$). The sub-matrix $\mathbf{K}_{II}$, $\mathbf{K}_{bb}$ in FE-BI denotes the self-interaction matrix in coating dielectric region, on the surface of coating dielectric respectively.

Method	MSDDM-FE-BI
Unknowns	5348
Memory of matrix $\mathbf{K}$	68.96 Mb($\mathbf{K}_{II}$)/46.5 Mb($\mathbf{K}_{bb}$)

Method	MSDDM-SVE-BI
Unknowns	3218
Memory of matrix $\mathbf{K}$	5.2 Mb($\mathbf{K}_{dd}$)/46.5 Mb($\mathbf{K}_{uu}$)

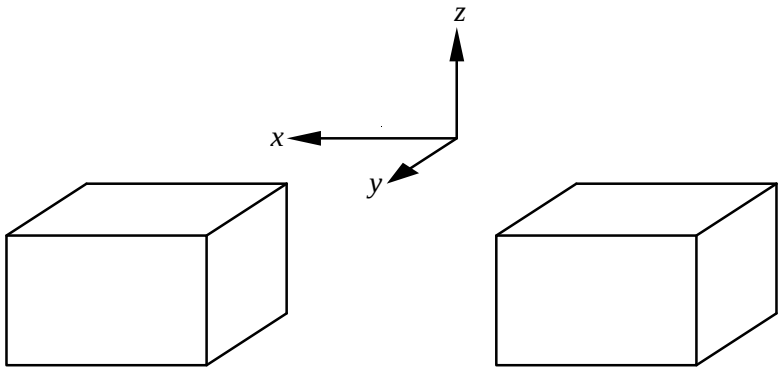

Figure 8. Two coating PEC cubes.

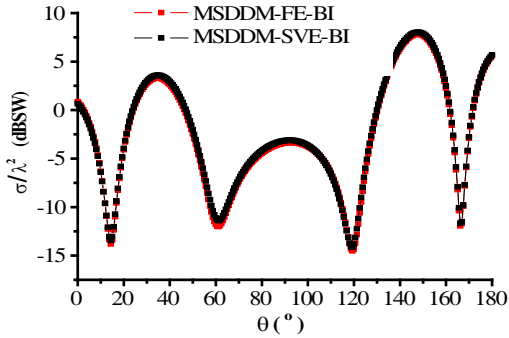

Figure 9. The bistatic RCS of two coating PEC cubes.

4.3. Two Coating PEC Cubes

The third example is two coating PEC cubes, shown in Fig. 8. The frequency is 300 MHz. The length of the cube is 0.5 m, the thickness of the coated layer is 0.02 m. The distance between the centers of two cubes is 1.6 m. The relative permittivity of coated layer $\varepsilon_r = 2.0$. The incident angle of plane wave is $\theta = 45°$, $\varphi = 0°$. The bistatic RCS results are shown in Fig. 9. The results by MSDDM-SVE-BI agree well with the one by MSDDM-FE-BI very well.

The comparisons of MSDDM-SVE-BI with MSDDM-FE-BI and DDM-FE-BI for this problem are demonstrated in Table 3. The total

Table 3. The comparison of MSDDM-SVE-BI with MSDDM-FE-BI and DDM-FE-BI. Bistatic RCS of two coating PEC cubes. (mesh density with $\frac{\lambda_0}{20}$). The sub-matrix $\mathbf{K}_{II}$, $\mathbf{K}_{bb}$ in FE-BI denotes the self-interaction matrix in coating dielectric region, on the surface of coating dielectric respectively.

Method	DDM-FE-BI	MSDDM-FE-BI
Total Unknowns	10688	10688
Memory of matrix K about single coating PEC cube	68.8 Mb ($\mathbf{K}_{II}$) 46.5 Mb ($\mathbf{K}_{bb}$)	68.8 Mb ($\mathbf{K}_{II}$) 46.5 Mb ($\mathbf{K}_{bb}$)
Computational time for matrix $\mathbf{X}_C$	29846.8 s	19711 s

Method	MSDDM-SVE-BI
Total Unknowns	6436
Memory of matrix K about single coating PEC cube	5.2 Mb ($\mathbf{K}_{dd}$) 46.5 Mb ($\mathbf{K}_{uu}$)
Computational time for matrix $\mathbf{X}_C$	7115 s

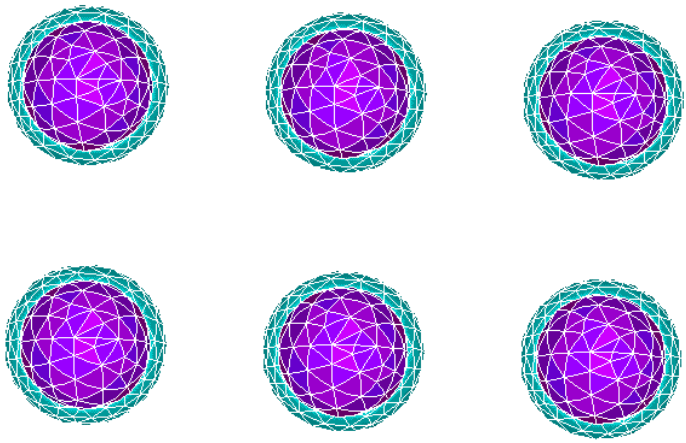

Figure 10. 3×2 array of coating PEC spheres.

Table 4. The comparison of MSDDM-SVE-BI with MSDDM-FE-BI and DDM-FE-BI. Bistatic RCS of 3×2 array of coating PEC spheres. (mesh density with $\frac{\lambda_0}{10}$). The sub-matrix $\mathbf{K}_{II}$, $\mathbf{K}_{bb}$ in FE-BI denotes the self-interaction matrix in coating dielectric region, on the surface of coating dielectric respectively.

Method	DDM-FE-BI	MSDDM-FE-BI
Total Unknowns	3138	3138
Memory of matrix K about single PEC coating sphere	0.81 Mb ($\mathbf{K}_{II}$) 0.33 Mb ($\mathbf{K}_{bb}$)	0.81 Mb ($\mathbf{K}_{II}$) 0.33 Mb ($\mathbf{K}_{bb}$)
Computational time for single matrix $\mathbf{X}_C$	22.4 s	8.7 s

Method	MSDDM-SVE-BI
Total Unknowns	1644
Memory of matrix K about single PEC coating sphere	0.051 Mb($\mathbf{K}_{dd}$) 0.33 Mb($\mathbf{K}_{uu}$)
Computational time for single matrix $\mathbf{X}_C$	3.2 s

unknowns are 6436, 10688, 10688 respectively for MSDDM-SVE-BI, MSDDM-FE-BI and DDM-FE-BI. The computational time for matrix $\mathbf{X}_C$ in MSDDM-SVE-BI, MSDDM-FE-BI and DDM-FE-BI is 7115 s, 19711 s, 29846.8 s respectively. Obviously, the advantage of MSDDM-SVE-BI for multiple conducting bodies coated by thin layer dielectric is remarkable.

4.4. 3×2 Array of Coating PEC Spheres

The fourth example is the scattering of 3×2 array of coating PEC spheres located in the x-y plane. The radius of PEC sphere is 0.2 m. The thickness of dielectric coating is 0.05 m with $\varepsilon_r = 2.0$, $\mu_r = 1.0$. The distance between the centers of two spheres is $0.8\lambda_0$ in both the x- and y-dimension as shown in Fig. 10. The excitation is $\hat{x}$ polarized plane wave propagating into the negative $\hat{z}$ direction at 0.3 GHz. Both the co-polarization and cross-polarization cases are evaluated.

As shown in Fig. 11(a), the results by MSDDM-SVE-BI also agree very well with the one of the Moment of Method (MoM), and the one of

MSDDM-FE-BI for co-polarization case. About the cross-polarization case, the results by MSDDM-SVE-BI also agree with the results by the MSDDM-FE-BI and DDM-FE-BI, from Fig. 11(b).

Table 4 demonstrates the comparisons between MSDDM-SVE-BI, MSDDM-FE-BI and DDM-FE-BI. In the MSDDM-FE-BI, the total number of unknowns is 3138, the computational time for single matrix $\mathbf{X}_C$ are 8.7 seconds, but in the MSDDM-SVE-BI, the total number of unknowns is only 1644, the computational time for single matrix $\mathbf{X}_C$ are only 3.2 seconds. To solve single matrix $\mathbf{X}_C$, traditional DDM-FE-BI requires computational time of 22.4 s.

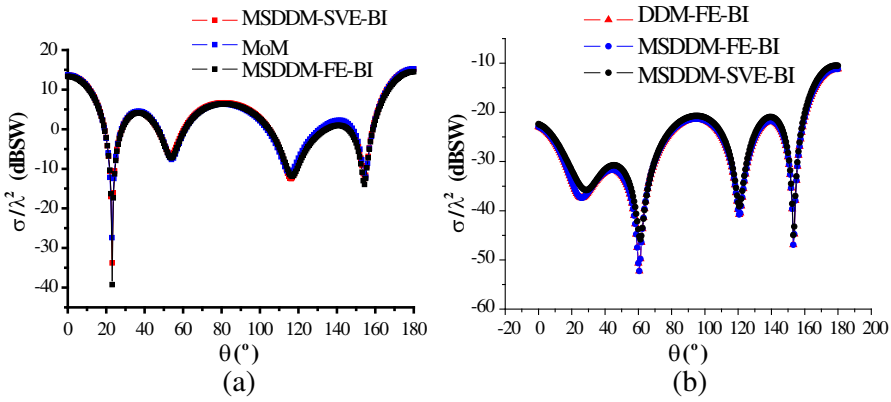

Figure 11. The bistatic RCS of 3×2 array of coating PEC spheres. (a) Co-polarization. (b) Cross-polarization.

Table 5. The comparison of MSDDM-SVE-BI ,MSDDM-FE-BI and DDM-FE-BI. Bistatic RCS of 5×5 array of coating PEC spheres. (mesh density with $\frac{\lambda_0}{10}$). The sub-matrix $\mathbf{K}_{II}$, $\mathbf{K}_{bb}$ in FE-BI denotes the self-interaction matrix in coating dielectric region, on the surface of coating dielectric respectively.

Method	DDM-FE-BI	MSDDM-FE-BI
Total Unknowns	13075	13075
Memory of matrix K about single coating PEC sphere	0.81 Mb ($\mathbf{K}_{II}$) 0.33 Mb ($\mathbf{K}_{bb}$)	0.81 Mb ($\mathbf{K}_{II}$) 0.33 Mb ($\mathbf{K}_{bb}$)
Computational time for matrix $\mathbf{X}_C$	560 s	207 s

Method	MSDDM-SVE-BI
Total Unknowns	6850
Memory of matrix K about single coating PEC sphere	0.051 Mb ($\mathbf{K}_{dd}$) 0.33 Mb ($\mathbf{K}_{uu}$)
Computational time for matrix $\mathbf{X}_C$	74 s

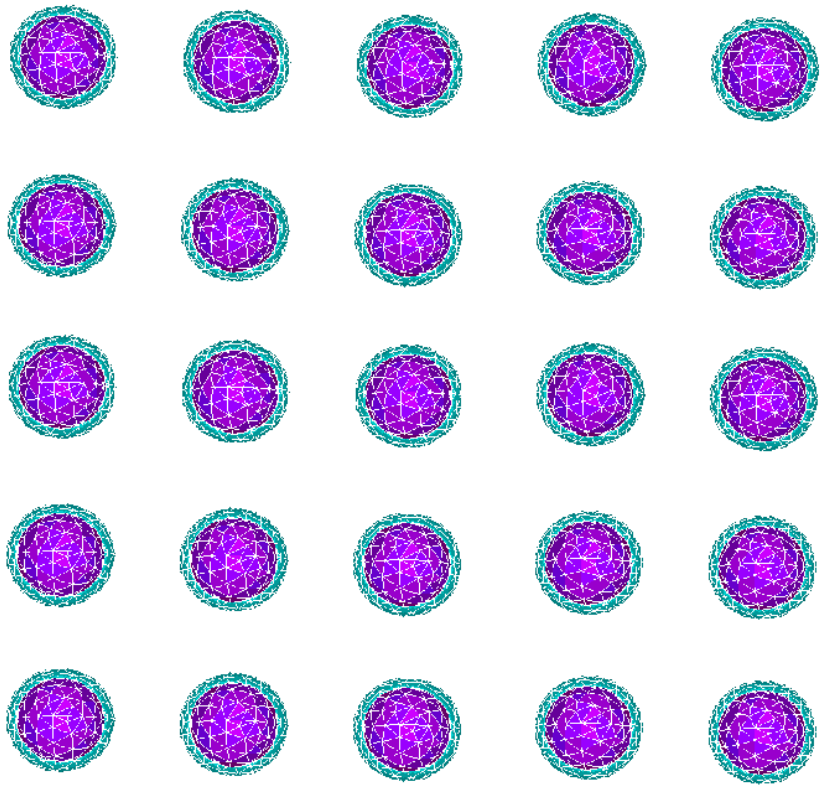

Figure 12. 5×5 array of coating PEC spheres.

4.5. 5×5 Array of Coating PEC Spheres

The fifth example is the scattering of 5×5 array of coating PEC spheres located in the x-y plane. The radius of PEC sphere is 0.2 m. The thickness of dielectric coating is 0.05m with $\varepsilon_r = 2.0$, $\mu_r = 1.0$. The excitation is $\hat{x}$ polarized plane wave propagating into the negative $\hat{z}$ direction at 0.3 GHz. The distance between the centers of two spheres

is $0.8\lambda_0$ in both the x- and y-dimension as shown in Fig. 12. Both the co-polarization and cross-polarization cases are evaluated.

As shown in Fig. 13(a), the results by the present method agree well with the results of MSDDM-FE-BI and DDM-FE-BI for the co-polarization case. About the cross-polarization case, as shown in Fig. 13(b), the results by MSDDM-SVE-BI does not agree so well with the results by the MSDDM-FE-BI and DDM-FE-BI, this is because the relatively weak interactions between elements of this array cannot be evaluated accurately by the SVE-BI method.

The comparison of MSDDM-SVE-BI, DDM-FE-BI and MSDDM-FE-BI is shown in Table 5. The Computational time for matrix $\mathbf{X}_C$ by DDM-FE-BI, MSDDM-FE-BI and MSDDM-SVE-BI are 560 s, 207 s, 74 s, respectively.

4.6. Two Coating PEC Spheres

The final example is the scattering of two coating PEC spheres located in the x-y plane, as shown in Fig. 14. The diameter of PEC sphere is 3.0 m. The thickness of dielectric coating is 0.02 m with $\varepsilon_r = 2.0 - j1.5$, $\mu_r = 1.0$. The excitation is $\hat{x}$ polarized plane wave propagating into the negative $\hat{z}$ direction at 0.3 GHz. The distance between the centers of two spheres is $3.5\lambda_0$. Both the co-polarization and cross-polarization cases are evaluated.

As shown in Fig. 15, the results by the present method agree well with the results of MSDDM-FE-BI both with the co-polarization and the cross-polarization. The total unknowns required by the MSDDM-

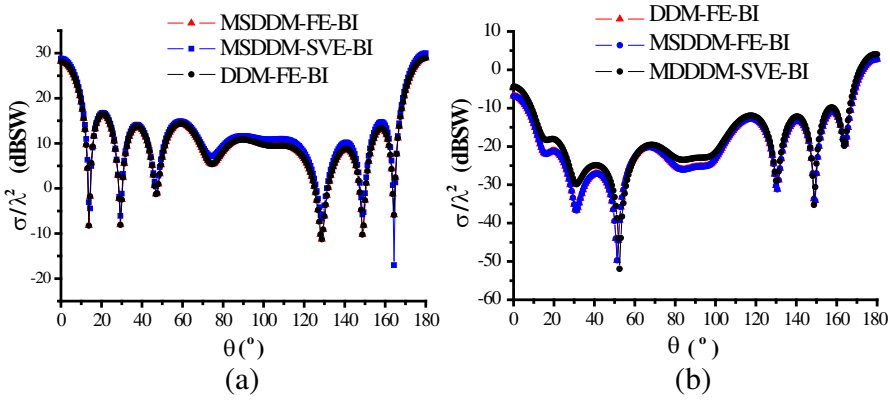

Figure 13. The Bistatic RCS of 5×5 array of coating PEC spheres. (a) Co-polarization. (b) Cross-polarization.

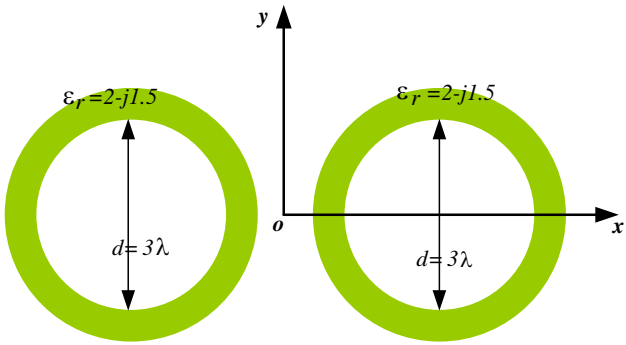

Figure 14. Two coating PEC spheres.

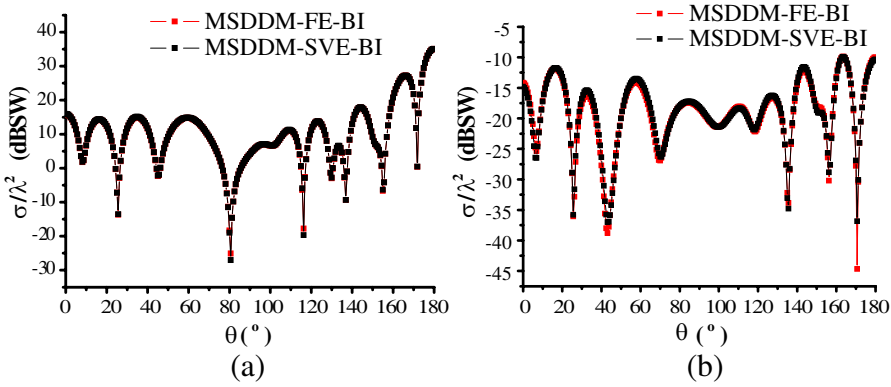

Figure 15. The bistatic RCS of two coating PEC spheres. (a) Co-polarization (b) Cross-polarization.

FE-BI and MSDDM-SVE-BI are 61652, 42746 respectively. The total storage requirement of the MSDDM-SVE-BI is nearly half of the one of the MSDDM-FE-BI. The above examples demonstrate the present method is very efficient for multiple PECs coated by thin materials.

5. CONCLUSIONS

In this paper, the matrix splitting domain decomposition method based on hybrid shell vector element–boundary integral (MSDDM-SVE-BI) is developed for analyzing multiple conducting bodies coated by thin layer dielectric. Compared with traditional tetrahedral elements, the shell vector elements reduce the number of unknowns greatly. Further, matrix splitting domain decomposition method based on a block

Gauss-Seidel type pre-conditioner is used for expediting the solution of connecting matrix. Based on this method, no iterative or inverse operation for the original SVE matrix is required, the computational time for connecting matrix can be reduced greatly. Typical numerical results show that MSDDM-SVE-BI is accurate, efficient method for electromagnetic scattering from multiple conducting bodies coated by thin layer dielectric.

Although the present method enhances the computational ability compared with DDM-FE-BI and MSDDM-FE-BI, fast algorithms are still required to incorporate into it for larger problems. Some direct methods like LU decomposition, hierarchical matrix method, and fast iterative algorithms like multilevel fast multipole algorithm (MLFMA) are appropriate choices. This work is in process.

ACKNOWLEDGMENT

This work is supported partly by NSFC (No. 60971032), the Programme of Introducing Talents of Discipline to Universities under Grant b07046. Thank valuable comments from anonymous reviewers.

REFERENCES

1. Zheng, H. X., X. Q. Sheng, and E. K. N. Yung, "Computation of scattering from anisotropically coated bodies using conformal FDTD," *Progress In Electromagnetics Research*, Vol. 35, 287–297, 2002.
2. Hu, X. J. and D. B. Ge, "Study on conformal FDTD for electromagnetic scattering by targets with thin coating," *Progress In Electromagnetics Research*, Vol. 79, 305–319, 2008.
3. Rao, S. M., C. C. Cha, R. L. Cravey, and D. L. Wilkes, "Electromagnetic scattering from arbitrary shaped conducting bodies coated with lossy materials of arbitrary thickness," *IEEE Trans. Antennas Propagat.*, Vol. 39, No. 5, 627–631, May 1991.
4. Jin, J. M., *The Finite Element Method in Electromagnetics*, John Wiley & Sons Inc, New York, 1993.
5. Jin, J. M. and J. L. Volakis, "A finite element-boundary integral formulation for scattering by three-dimensional cavity-backed apertures," *IEEE Trans. Antennas Propagat.*, Vol. 39, 97–104, Jan. 1991.
6. Ali, M. W., T. H. Hubing, and J. L. Drewniak, "A hybrid FEM/MoM technique for electromagnetic scattering and radiation

from dielectric objects with attached wires," *IEEE Trans. Electromag. Compat.*, Vol. 39, 304–314, Nov.1997.

7. Sheng, X. Q., J. M. Jin, J. Song, C. C. Lu, and W. C. Chew, "On the formulation of hybrid finite-element and boundary-integral methods for 3-D scattering," *IEEE Trans. Antennas Propagat.*, Vol. 46, 303–311, Mar. 1998.
8. Wang, D. S., "Limits and validity of the impedance boundary condition on penetrable surfaces," *IEEE Trans. Antennas Propagat.*, Vol. 35, 453–457, Apr. 1987.
9. Lu, C. C., "A modified thin dielectric approximation for calculation of EM scattering by dielectric objects with thin material coating," *IEEE Antennas and Propagation International Symposium*, 2809–2812, Jun. 9–15, 2007.
10. Chiang, I. T. and W. C. Chew, "A coupled PEC-TDS surface integral equation approach for electromagnetic scattering and radiation from composite metallic and thin dielectric objects," *IEEE Trans. Antennas Propagat.*, Vol. 54, 3511–3516, 2006.
11. Pan, G. and R. M. Narayanan, "Electromagnetic scattering from a dielectric sheet using the method of moments with approximate boundary condition," *Electromgnetics*, Vol. 24, No. 5, 369–384, Jul. 2004.
12. He, S., Z. Nie, and J. Hu, "Numerical solution of scattering from thin dielectric-coated conductors based on TDS approximation and EM boundary conditions," *Progress In Electromagnetics Research*, Vol. 93, 339–354, 2009.
13. He, S., Z. Nie, J. Wei, and J. Hu, "Numerical solution for dielectric-coated PEC targets based on multi-layer TDS approximation", *Microwave Conference Proceedings & Asia-Pacific Conference Proceedings*, 2008.
14. He, S., Z. Nie, J. Wei and J. Hu, "A highly efficient numerical solution for dielectric-coated PEC targets," *Waves in Random and Complex Media*, Vol. 19, No. 1, 65–79, Feb. 2009.
15. Ren, Z., "Degenerated prism elements-general nodal and edge shell elements for field computation in thin structures," *IEEE Trans. Magnetics*, Vol. 34, No. 5, 2547–2550, Sep. 1998
16. Abenius, E. and F. Edelvik, "Thin sheet modeling using shell elements in the finite-element time-domain method," *IEEE Trans. Antennas Propagat.*, Vol. 54, No. 1, 28–34, Jan. 2006.
17. Lei, L., J. Hu, and H. Q. Hu, "Solving scattering from conducting body coated by thin-layer material by hybrid shell vector element with boundary integral method," *International*

Journal of Antennas and Propagation, Vol. 2012, 1–9, 2012.

18. Ilić, M. M. and B. M. Notaro, "Higher order FEM-MoM domain decomposition for 3-D electromagnetic analysis," *IEEE Antenna and Wireless Propagation Letters*, Vol. 8, 970–973, 2009.
19. Cui, Z. W., Y. P. Han, X. Ai, and W. J. Zhao, "A domain decomposition of the finite element-boundary integral method for scattering by multiple objects," *Electromagnetics*, Vol. 31, 469–482, 2011.
20. Zhao, K. Z., "A domain decomposition method for solving electrically large electromagnetic problems," Dissertation of Ph.D., The Ohio State University, 2007.